Imperial College London
Department of Earth Science and Engineering
MSc in Environmental Data Science and Machine Learning

Independent Research Project
Final Report

# Machine Learning-Based Multi-Factor Modeling of Reef Island Shoreline Dynamics in the Maldives

by

Yiyu Yang

Email: yiyu.yang24@imperial.ac.uk
GitHub username: esemsc-yy1824
Repository: https://github.com/ese-ada-lovelace-2024/irp-yy1824

Supervisors:
Dr. Yves Plancherel
Prof. Matthew Piggott

September 2025

## ABSTRACT

Reef islands of the Maldives are low-lying accumulations of biogenic carbonate sediment whose shorelines respond to interacting oceanographic, climatic, and geomorphic drivers. Predicting shoreline change for reef islands is essential for risk-informed coastal planning. Historical shorelines cross nine years on six natural coral reef islands in South Maalhosmadulu Atoll are assembled in this study. Nine machine learning approaches are developed that predict dynamical along-transect shoreline position based on multi-source predictors and the hybrid transect framework method for minimizes satellite imaginary noise. From island-individual experiments, the stacking model (ensemble LightGBM, XGBoost, Ridge Regression) shows the highest performance with average $R^2$ value of 0.96 of all islands on test set. In Cross-Island Training, Random Forest surpasses all other models and achieved $R^2$ approximately 0.95 in the test set. Under the future prediction scenario, models trained on 2016–2023 accurately predict 2024 shoreline positions, with Random Forest achieving the $R^2$ value of approximately 0.94. Random Forest and Stacking both show good performance in single-island modeling, multi-island modeling, and future island morphology prediction. However, compared with Stacking and other models that use 5 MB or less memory, Random Forest requires more than 384 times that amount. Coral reef topography and local terrain slope are indicated as dominant predictors in island shape modeling, suggesting geomorphic controls on local shoreline dynamics. However, model evaluation on unseen islands shows the limitation of the cross-island generalization ability.

# 1. INTRODUCTION

The Maldives is a 750 km long archipelago in the central Indian Ocean, consisting of a double chain of 22 atolls that extend from 6°57′N to 0°34′S (Kench, McLean et al. 2005). Atoll islands occur in the tropics and are wave-built accumulations of carbonate sediment derived from the decomposition of calcium carbonate-secreting organisms that dwell on the adjacent, ring-shaped coral reef system (Masselink, Beetham et al. 2020, Barnett, Jarillo et al. 2022). These islands are ecologically important, which are the only naturally habitable land in atoll nations, such as the Maldives Islands (Kench, Sengupta et al. 2024).

A defining feature of atoll islands is their low elevation, often less than 1–2 m above high tide level, which makes them highly sensitive to fluctuations in surrounding environmental conditions (Roelvink, Masselink et al. 2025). Some previous projections, such as flood risk assessments, have assumed static morphology and no capacity for adjustment in island shape or elevation (Storlazzi, Gingerich et al. 2018, Wandres, Espejo et al. 2024). But in reality, atoll islands are highly dynamic landforms shaped by complex interactions among oceanographic, climatic, and geomorphological factors. They increase elevation through overwash processes, where waves transport sediments from reef flats and island shorefaces onto the island surface, contributing to vertical accretion in response to sea-level rise (Masselink, McCall et al. 2021). Different from other shoreline types, the hydrodynamics of reef islands are affected by spatial distribution and geomorphology of reef platforms, which makes them challenging for statistical analysis. Therefore, quantification of current reef island shape is highly reliant on direct anthropogenic records with climatic or human-caused events that cause direct or indirect impact.

Previous researchers attempted to find the statistical correlations between the island shape change, environmental drivers (e.g., sea-level rise and wave energy), and the morphological features for coral reefs and islands (e.g., island orientation and reef width). Although they achieved high-quality and resolution data, the simplistic statistical approaches they've used fail to verify any robust correlation between the direct or potential impactors and the coral reef shoreline shape. The computationally robust non-linear models are required for incorporating multiple predictors about the shorelines of reef islands (Sengupta, Ford et al. 2023).

Remote sensing and machine learning techniques have significantly advanced image-based shoreline monitoring (Park and Song 2024, Christofi, Metas et al. 2025). The CoastSat has enabled the systematic extraction of shoreline positions from multispectral satellite imagery (Vos, Splinter et al. 2019). To date, no prior study has systematically developed and tested machine learning frameworks for predicting coral reef island shapes across multiple reef islands in the Maldives. This study addresses the gap by quantitatively characterising seven kinds of driving factors, developing the hybrid transect-based framework, and employing nine regression machine learning models and artificial neural networks to enhance the predictive capacity from external environmental drivers and local shoreline attributes. These projections offer insights into the sensitivity of island morphology to multiple environmental features, providing a basis for supporting local communities in implementing long-term monitoring programs.

# 2. METHODOLOGY

## 2.1. Research Region

This study focuses on six vegetated and uninhabited sand cays within the South Maalhosmadulu Atoll, Maldives (Figure 1), from 2016 to 2024. The islands are distributed across distinct atoll positions: east-north (Madhirivaadhoo), east-south (Aidhoo), centre (Keydhoo, Funadhoo), west (Dhakendhoo), and south (Mendhoo). Their landforms represent long-term natural evolution. This spatial distribution enables analysis of shoreline response variations associated with differences in exposure to wave energy and seasonal monsoon wind orientation across the atoll. These islands have limited direct human modification, making them suitable case studies for natural shoreline dynamics. Historical storm records from 2016 to 2024 report no extreme events (e.g., typhoons, cyclones) that would directly affect the shoreline configurations, ensuring that observed changes primarily result from oceanographic and geomorphological processes.

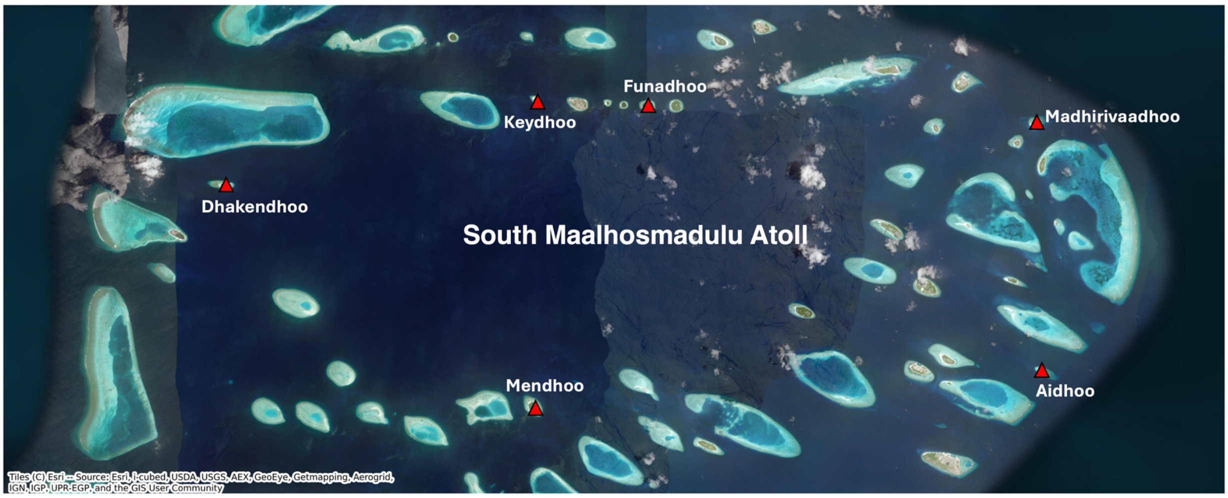


**Figure 1.** Locations of the experimental coral reef islands in the South Maalhosmadulu Atoll, Maldives, with each red triangle representing one island.

Tropical maritime climate brings persistent cloud cover, significantly reducing the availability of satellite imagery required for shoreline extraction, which is the main challenge in data acquisition of the Maldives. As a result, extracted shoreline observations are temporally irregular rather than evenly distributed.

The shoreline segment serves as the research unit. To ensure that the model analysed general mechanisms rather than differences among islands, distinguishing features such as area and perimeter were excluded from the analysis. Sentinel-2 imagery, available since 2016, defines the temporal scope as 2016 to 2024. Due to this relatively short period, sea-level rise was not explicitly modelled.

## 2.2 Multi-source Data Acquisition

### 2.2.1. Satellite Remote Sensing Data: Sentinel-2 and Landsat 8/9

Shoreline positions from 2016 to 2024 were extracted from the satellite imagery with 10-meter spatial and 5-day temporal resolution by the CoastSat with manual verification. And the hybrid transect framework (described in Section 2.2) was employed to transform morphological data into numerical representations. For each shoreline acquisition date, the

Normalised Difference Vegetation Index (NDVI) was computed to capture vegetation cover across the reef islands.

$$NDVI = \frac{NIR - Red}{NIR + Red} \qquad (1)$$

For Sentinel-2, Band 8 (842 nm) and Band 4 (665 nm) were used, while for Landsat 8/9, Band 5 (865 nm) and Band 4 (655 nm) were adopted. All imagery was atmospherically corrected (Level-2 products). For each acquisition, the median NDVI within the island footprint was recorded and assigned to all shoreline segments of that island. For the NDVI unavailable date, a ±5-day tolerance temporal window was applied for these occasional data gaps by using the nearest available NDVI value.

Island morphology reflects the interaction of biological sediment production and hydrodynamic forcing, which drive both island formation and continuous sediment redistribution along reef shorelines (Kench, Brander et al., 2009; Kench, Beetham et al., 2017). And to avoid inputting features that could trivially differentiate islands (e.g., island area or perimeter), island orientation is the only morphological descriptor used via principal component analysis (PCA).

### 2.2.2. NASADEM

The beach width and slope of Maldivian islands varies significantly around the islands (Kench and Brander 2006).To estimate coastal topographic slopes landward of the shoreline, the NASADEM digital elevation model are utilised with 30-meter resolution. For each transect and available date, the shoreline position was identified, and a 40-meter landward segment was extracted along the transect line. Elevation values were sampled at 5-meter intervals, converted to geographic coordinates, and filtered to ensure they include the valid spatial extent of the DEM. Elevation values were extracted from the NASADEM dataset using bilinear interpolation. The shoreline slope was calculated as the difference between the maximum and minimum elevation values along the sampled profile, divided by the corresponding horizontal distance. This results in an average slope in meters per meter. Transects with fewer than two valid elevation values or with no elevation variation were excluded. This approach generated shoreline-perpendicular slope estimates for each transect and enabled analysis of topographic dynamics in the nearshore zone.

### 2.2.3. Wind and Wave Reanalysis Data from ECMWF

Wind characteristics in the Maldives are closely linked to monsoon type (Section E). Long-term records since 1964 show that the Hulhangu monsoon (from April to November) is dominated by west to northwest winds (~225°–315°) with a mean speed of 5.1 m $s^{-1}$. In contrast, the Iruvai monsoon (from December to March) is driven by east to northeast winds (~45°–90°) with a mean speed of 4.9 m $s^{-1}$. These two monsoon systems produce strong seasonal reversals in wind direction, though within a relatively narrow angular range. Wind speed is most variable during the transitional period between the two monsoons, with mean speed dropping to 3.5 m $s^{-1}$ in March. Climate records for the study period (January 2002–February 2003) indicate that wind direction and speed were consistent with long-term averages (Meteorology 1995).

Wave climate data for the Indian Ocean surrounding the Maldives show that dominant swells primarily approach from southerly directions. Seasonally, swells from the south-southwest prevail from April to November, with a peak significant wave height (Hs) of 1.8 m in July. From December to March, swells shift to the southeast, with a minimum mean Hs of 0.75 m in March. Wave data from gauges placed on the windward reef edge of islands across the whole atoll during 2002 and 2003, which reveals distinct wave energy gradients with the shift pattern between monsoon seasons. Overall, wave energy was highest during the westerly monsoon, which showed the greatest reduction across the atoll. During this period, Hs at the windward reef edge decreased by up to 0.7 m from the western (Dhakendhoo) to the eastern islands. A reverse gradient was observed during the northeast Iruvai monsoon, with Hs reducing by 0.27 m from east to west (Young 1999).

This study considered nearshore wind and wave conditions by using ERA5 reanalysis data from the European Centre for Medium-Range Weather Forecasts (ECMWF) through the Copernicus Climate Data Store. The analysis included significant wave height, mean wave period, and the 10-meter u and v components of wind. The dataset is provided at a spatial resolution of 0.25° × 0.25°, covering the study site's bounding box and corresponding to all available dates in the shoreline slope time series.

For each month with valid shoreline observations, the study downloaded and processed daily ERA5 data. At each transect location, the nearest ERA5 grid point was identified using a KDTree nearest-neighbour search. The study then constructed time series of environmental conditions for each transect by extracting variable values at the matched grid locations for each available time step.

This procedure produced a dataset that matched wave and wind conditions to each shoreline transect in both space and time. This alignment enabled joint analysis of physical forcing and shoreline dynamics.

#### 2.2.4. The Improved Gridded Bathymetric Data

Local-scale geomorphology plays a crucial role in shaping sediment transport pathways and the subsequent shoreline patterns of accretion or erosion (Kench and Brander 2006, Ortiz and Ashton 2019, Shope and Storlazzi 2019, Wu, Duvat et al. 2021). The islands focused on this study are formed from sand-sized sediments deposited directly on the reef surface, which ensures active interaction with contemporary reef platform processes. Although the islands are relatively small and broadly similar in scale, they occupy different proportions of the reef platform, creating variations in their local-scale geomorphic setting and environmental exposure.

In contrast to previous studies that rely on remote sensing imagery to detect reef width and position (Sengupta, Ford et al. 2023), this study utilizes high-resolution bathymetric data from the Maldives to quantify reef structure along transects. This approach mitigates the issue of persistent cloud cover in tropical regions and enables analysis of additional features, including reef crest elevation and reef slope. The analysis is based on the improved gridded bathymetry data set developed by Shuaib Rasheed for the Maldives (Rasheed, Warder et al. 2021).

For each shoreline segment, a 1 km radial search identified surrounding bathymetric data points. The reef crest was defined as the shallowest point, representing the highest elevation in the sea area within this buffer. Reef width was calculated as the geodesic distance between the shoreline point and the reef crest.

A linear profile was then sampled between the shoreline and the reef crest. Using interpolated bathymetric values along this profile, we computed the mean depth of the reef flat. The reef slope was estimated as the angle (in degrees) derived from the elevation difference between the shoreline and reef crest, normalised by the reef width.

### 2.2.5. Monsoon Classification

The Maldives experience two monsoon periods marked by strong seasonal reversals in wind direction, shifting from the west-northwest to the northeast. Morphological responses of reef island beaches and shorelines to these predictable shifts were examined on eight islands in South Maalhosmadulu Atoll during 2002 and 2003. Previous field surveys revealed that substantial seasonal changes in shoreline position, with gross variations ranging from 31% to 120% of the total beach area. These fluctuations are linked to large reversals in sediment transport, on the order of $9–23 \times 10^3$ $m^3$ per season, driven by alternating wind and wave conditions. Despite these large seasonal shifts, the annual net change remained relatively small (2–15%), indicating that the islands operate within a dynamic equilibrium system.

Island geometry is a stronger predictor of morphological change than wave energy exposure. Shoreline variability is directly influenced by the two dominant monsoon systems: Hulhangu (Southwest Monsoon) and Iruvai (Northeast Monsoon) systems, which drive seasonal reversals in prevailing wind directions (Kench and Brander 2006). Consequently, monsoon classification and island geometry, as discussed in Section x, are critical for accurately modeling sediment transport patterns in these islands.

## 2.3. Hybrid Transect Framework

In this study, shoreline extraction will be performed using the CoastSat toolkit, an open-source Python package that leverages Google Earth Engine to retrieve and process time-series shoreline positions from Landsat and Sentinel-2 satellite imagery (Vos, Splinter et al. 2019).

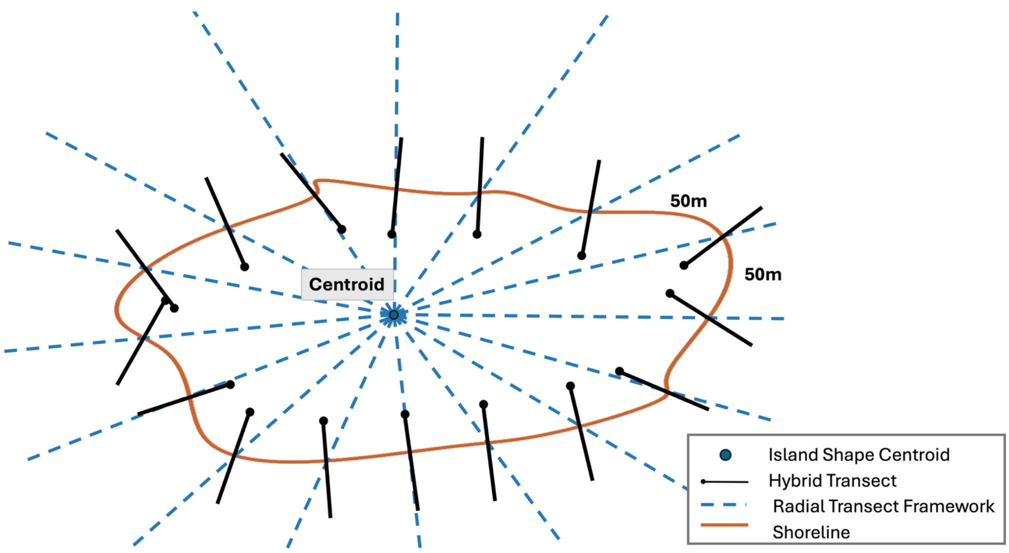


**Figure 2.** The hybrid transect framework and its construction principle. Radial transects are drawn from the centroid so that shoreline intersection points are spaced about 50 meters apart, rather than evenly angled.

CoastSat delineates shorelines as discrete points. One common method is to connect these points into a polygon and generate vertical transects at fixed intervals. This approach, however, is susceptible to noise from detection errors such as cloud contamination or the presence of nearby islands in the satellite imagery, especially in tropical regions where cloud noise is particularly strong. An alternative method involves generating evenly spaced transects radially from the shoreline centroid and measuring the distance to the nearest intersection point, which produces a more continuous representation. However, the resulting transects are not perpendicular to the local shoreline, causing the measured shoreline change direction to differ from the actual physical forces acting on it. This misalignment introduces systematic errors when attempting to capture wave and wind forcing.

The hybrid transect framework is constructed by first estimating the tangent direction of a reference shoreline, and then placing perpendicular transects at equal arc-length intervals along the shoreline. Radial rays are generated from the island centroid to establish uniform angular spacing. At each intersection of a radial transect with the shoreline, a perpendicular transect is constructed using the local tangent direction of the shoreline. This approach ensures that transects consistently capture cross-shore distances, reduces orientation bias, and automatically excludes small offshore islets and noise polygons.

To improve the cross-island generalization ability of the model, this study normalizes the shoreline position into a dimensionless unit and introduces the island-scale factor $R_{mean}$ to eliminate the influence of different island sizes on prediction. First, based on remote sensing imagery, the shoreline position $d(T)$ (in meters) of each transect is corrected for tide level. The year 2016 is selected as the reference year, and the earliest valid observation of that year is taken as the baseline $\mathrm{d}_0(T)$. Then, calculating the average length of all line segments from the centroid to the shoreline along the transects in the reference year to obtain the island-scale factor $R_{mean}$, representing the characteristic radius of the island. Finally, the absolute shoreline change distance is calculated and normalized into the dimensionless change $\Delta d_t{}'(T)$, which is used as the training target of the model. This eliminates the effect of island size and makes the prediction results among different islands comparable.

$$R_{mean} = median(d_0(T_1), d_0(T_2), \dots, d_0(T_n)) \tag{2}$$

$$\Delta d_t{}'(T) = \frac{d_t(T) - d_0(T)}{R_{mean}} \tag{3}$$

$\mathrm{d}_0$represents the reference year, $T$ represents all transects, $T_n$ represents the transect with index n, $R_{mean}$ is the island-scale factor, and $\Delta d_t{}'(T)$ represents the dimensionless change value of the recorded shoreline.

Additionally, although some studies pointed out that reef islands may experience overall positional shifts under the influence of ocean currents. But such changes are generally slow and long-term, which makes their impact negligible within the nine years covered by the available satellite data period, and therefore not further considered in this study.

## 2.4. Tidal Correction

Given that satellite imagery only captures instantaneous shoreline positions that are sensitive to tidal stage, shoreline positions require correction by the tidal model. FES2022 tidal model integrates hydrodynamic modeling with satellite altimetry and tide gauge assimilation. This study utilizes FES2022 (LEGOS 2024) to adjust observed shoreline positions to mean tidal conditions to reduce tidal bias.

## 2.5. Multi-factor Machine Learning Model

The Maldives is in a tropical region where persistent cloud cover frequently obscures satellite imagery, often concealing substantial portions of coastlines or even entire islands. So shorelines extracted from satellite observations do not form evenly spaced time series. To accommodate this temporal irregularity, sequence-based models such as LSTMs were not employed. Instead, regression-based approaches were adopted to capture the relationships between shoreline morphology and multiple environmental predictors.

The models evaluated in this study include ensemble methods (Random Forest, LightGBM, XGBoost, Stacking), a linear model (Ridge Regression), an instance-based method (K-Nearest Neighbours), and neural networks (Multi-layer Perceptron Regressor, feed-forward neural networks, and auto-tuned variants). Stacking refers to a meta-model that combines predictions from LightGBM, XGBoost, and Ridge Regression. Preliminary investigations suggest that there is currently no dedicated machine learning model specifically tailored for predicting future island area changes in the Maldives. To address this gap, this study proposes a unified predictive pipeline that integrates multiple forcing factors (including tidal variability, seasonal monsoon dynamics, and local geomorphic controls) within machine learning approaches and neural networks.

Model validation used rolling-window and cross-validation schemes applied to historical observations to ensure robustness and generalizability. Performance was assessed using the coefficient of determination ($R^2$), root mean square error ($RMSE$), and mean squared error ($MSE$), which are defined as follows:

Coefficient of Determination ($\mathrm{R}^2$):

$$R^2 = 1 - \frac{\sum_{i=1}^{n}(y_i - \hat{y}_i)^2}{\sum_{i=1}^{n}(y_i - \bar{y})^2} \tag{4}$$

Root Mean Squared Error (RMSE):

$$RMSE = \sqrt{\frac{1}{n}\sum_{i=1}^{n}(y_i - \hat{y}_i)^2} \tag{5}$$

Mean Squared Error (MSE):

$$MSE = \frac{1}{n}\sum_{i=1}^{n}(y_i - \hat{y}_i)^2 \tag{6}$$

Where $y_i$ represents the observed values, $\hat{y}_i$ represents the predicted values, $\bar{y}$ is the mean of the observed values, and $n$ is the total number of samples.

## 3. RESULT

In the experiments where six reef islands of South Maalhosmadulu Atoll are modelled, trained, and tested separately, the $R^2$ results under nine machine learning approaches are shown in Figure 3. In all experiments, the shoreline segments within the data range were randomly divided into training and validation sets, with a fixed ratio of 8:2. From the training results, the stacking model (ensemble of LightGBM, XGBoost, and Ridge Regression) achieves the highest mean $R^2$ of 0.962 across the six islands. The next best is Random Forest and XGBoost, both with mean $R^2$ values close to 0.955. Overall, ensemble learning models perform the best among all model types, followed by the neural network with automatic parameter tuning. On the other hand, Ridge Regression, KNN and MLP regressor show very poor performance across all islands, with all mean $R^2$ close or below 0.5.

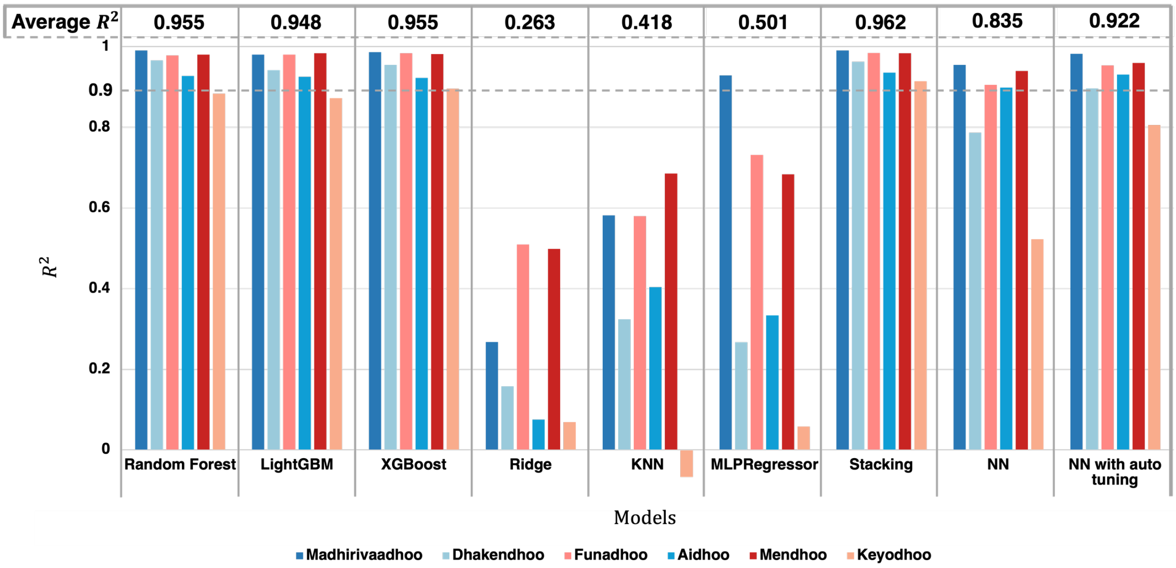


**Figure 3.** Comparison of $R^2$ values for six natural reef islands in South Maalhosmadulu Atoll under nine common machine learning approaches, with the mean $R^2$ of each model representing its overall fitting performance. NN refers to neural network, and this abbreviation is consistently applied in the subsequent discussion

To evaluate the predictive ability of models compatible with shoreline dynamics across all islands, experiments were conducted by training and testing the models on the combined dataset of all six natural reef islands. The nine-year dataset was fully mixed in terms of time, island source, and shoreline segments, and the same nine models were applied for training. As shown in Figure 4, Random Forest achieved the highest $R^2$ value of 0.95 with the lowest MSE and RMSE values. In addition, the stacking model and the auto-tuned neural network also show $R^2$ values higher than 0.9, but at the cost of relatively longer training time.

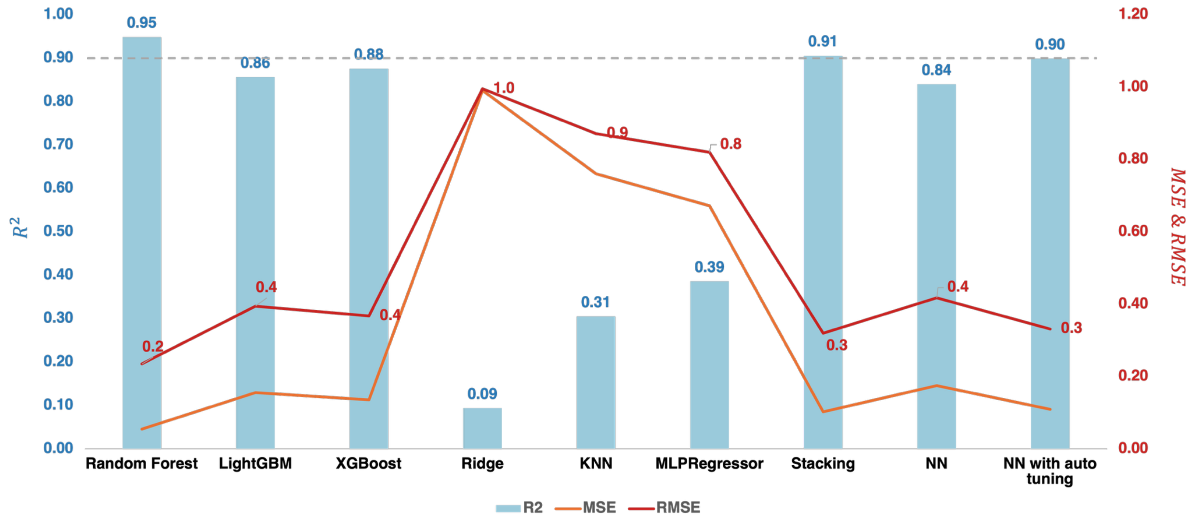


**Figure 4.** $R^2$ and RMSE performance of nine models on the combined dataset of all islands. Blue bars represent $R^2$ values, and the red line indicates RMSE values.

To evaluate the transfer performance of these nine models on islands they had never encountered before, the experiment conducted prediction on Keyodhoo and used the remaining five islands for training. As observed (Figure 5), for the five training islands, the test $R^2$ values of ensemble learners and neural networks are near and above 0.9. However, when applied to the unseen island, all models produced bad $R^2$ values which lower than 0.2 and even showing string negative values in neural networks.


**Figure 5.** $R^2$ values of nine models trained and tested on data from five islands and applied to predict the remaining unseen island.

To evaluate predictive performance under future scenario, models were trained on shoreline shape data from 2016 to 2023, and data from 2024 which represent future states of the previous shorelines. As shown in Figure 6 and Table 1, Random Forest still delivers the best overall performance across the indicators $R^2$, MSE, and RMSE, each reaching $R^2$ values above 0.94 on both the 2016-2023 test set and the 2024 prediction data. At the same time, neural networks show very poor prediction ability, similar to the previous experiment, and even performs much worse than simple statistical methods such as KNN and Ridge Regression.


**Figure 6.** $R^2$ values of models trained on 2016–2023 shoreline data and applied to predict the "future" shoreline state in 2024.

**Table 1.** Comparison of $R^2$, MSE, and RMSE values for seven models trained on 2016–2023 data and used to predict shoreline states in 2024 (shown to two significant figures).

| | $R^2$ | | MSE | | RMSE | |
|---|---|---|---|---|---|---|
| Model | Test | Prediction | Test | Prediction | Test | Prediction |
| **Random Forest** | **0.95** | **0.94** | **0.05** | **0.00** | **0.22** | **0.06** |
| **LightGBM** | 0.83 | 0.79 | 0.16 | 0.01 | 0.41 | 0.11 |
| **XGBoost** | 0.87 | 0.82 | 0.13 | 0.01 | 0.36 | 0.10 |
| **MLP Regressor** | 0.09 | 0.08 | 0.89 | 0.05 | 0.95 | 0.23 |
| **Stacking** | 0.29 | 0.25 | 0.69 | 0.04 | 0.83 | 0.20 |
| **Neural Network** | 0.22 | 0.17 | 0.76 | 0.05 | 0.87 | 0.21 |
| **Neural Network (with auto tuning)** | 0.91 | 0.88 | 0.08 | 0.01 | 0.29 | 0.08 |

In addition to their high predictive accuracy, the ensemble learning models also required much less training time compared with the neural network, whose performance ranked just above them. Among them, Random Forest shows the best or second-best performance in multi-island and future prediction. However, the overall size of its model and parameters takes at least 469.6 MB of memory, which is more than 384 times the average memory usage of other models (no more than 5 MB).

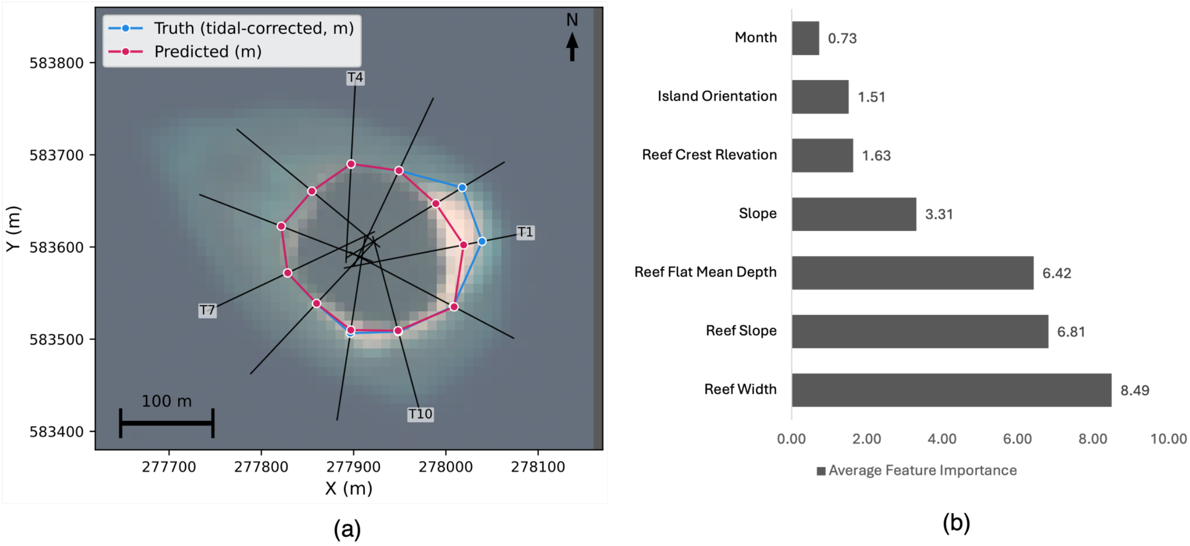


**Figure 7.** (a) Difference between model predictions and ground truth for one reef island in 2024-12-11 in 2024 by the Stacking model. (b) Feature importance statistics showing the average contribution of each input variable to the model predictions.

The prediction result of Keyodhoo on 2024-12-11 is shown in Figure 7(a). The blue line represents the ground truth shoreline shape after tidal correction of the extracted shoreline in the background satellite imagery using the FES2022 model. The magenta line represents the shoreline predicted by the stacking model. The corresponding $R^2$, MSE, and RMSE values of this prediction are 0.93, 0.01, and 0.11, respectively. As can be seen from the figure, except for two points with relatively obvious deviations, most of the other points almost overlap with the ground truth.

Feature importance analysis (b in Figure 7) shows the average contribution of each input feature to the model outputs, based on all experiments above on the nine models. In each experiment, the feature importance of each model was normalized before being accumulated across models to ensure comparability. It reveals that reef-related characteristics (e.g., reef width, slope and flat depth) and local terrain slope are the dominant contributors to predictive performance, highlighting the crucial role of reef geomorphology in affecting shoreline dynamics. Local terrain slope, which reflects the local patterns of sediment transport and accumulation, accounted for nearly 10% of the predictive contribution. And reef width that influence wave energy and wind-driven shoreline processes together account for approximately 26%. Within the research period, the islands in the Maldives did not experience major storms or other extreme events, and thus shorelines were not subjected to conditions of heightened wind or wave forcing. If the study period were to include extreme storm events, the strong impacts of wind and waves under some specific conditions would need to be considered separately from those observed under normal climatic conditions.

# 4. DISCUSSION

**Single Island Experiment**
From the experiments on the six individual natural reef islands, tree-based ensemble learners such as Random Forest are relatively the most effective model types for capturing the high-dimensional relationships between multiple influencing factors (e.g., climate and topography) and local shoreline positions. The Stacking model shows the highest performance among all models, which comes from the advantage of integrating different ensemble algorithms when combining multiple models. Random Forest and XGBoost follow closely, showing the strength of tree-based ensemble methods in capturing the multi-factor driven patterns of shoreline dynamics. Although neural networks are slightly weaker than ensemble learning and rely on parameter tuning, they still perform better than most traditional methods. In contrast, KNN and Ridge Regression consistently show very poor predictive performance, which indicates that the input–output relationships in shoreline prediction are strongly nonlinear and complex. This also explains why traditional linear statistical approaches in earlier studies failed to effectively fit shoreline behaviour.

**Multiple Island Experiment**
In the experiment where the model was trained and tested using data from all islands, the Random Forest showed the best performance, followed by Stacking and the parameter-tuned Neural Network. These three models were still able to keep test $R^2$ values above 0.9 in the multi-island experiment. However, compared with the single-island experiment, the performance of LightGBM and XGBoost dropped significantly.

**Cross-Island Generalization Experiment**
When applying machine learning approaches to predict islands that were never included during training, large deviations between predicted and observed shorelines were found. This means that the patterns learned from the five islands are not sufficient to generalize to a new island, even though all six belong to the same atoll. For neural networks, which strongly rely on large data, the prediction performance was especially poor. This limitation mainly reflects that the driving mechanisms of island evolution may have clear regionality and non-stationarity and cannot be simply extrapolated by a single model.

**Future Scenario Prediction Experiment**
In the experiment predicting future shoreline states (2024) based on data from 2016–2023, the ensemble learners showed only a small drop in accuracy, with $R^2$ values decreasing by only 0.05 compared with the test results. In particular, Random Forest demonstrated stronger learning and prediction ability than the other seven models. This demonstrates that after fitting eight consecutive years of data, the ensemble models still maintain the ability to predict the morphodynamical changes of the ninth year, even though the shoreline data and model setup were not strictly time-series.

**Major Contributing Features**
Analysis of feature contributions across all experiments reveals that local terrain slope and reef width contribute more than all other feature types. This indicates that the most influential factors driving natural reef island shoreline morpho dynamics are the structural forms of the island and the reef platform (Sengupta, Ford et al. 2025). Due to the influence of the reef platform, shorelines are not directly exposed to the open ocean, which causes wind and wave energy to reach the adjacent coast in more complex forms. Local terrain slope affects the rate

and pattern of sediment transport and deposition, and also influences the erosion rate of seawater in the direction perpendicular to the shoreline (Shope and Storlazzi 2019). The impacts of these two variables are consistent with physical principles that shape shoreline morphology.

**Strengths and Limitations**

Overall, in terms of model accuracy across single-island, multi-island, and future prediction experiments, as well as in terms of training time consumption, Random Forest seems to be the best choice. However, one drawback that cannot be ignored is that its memory usage is more than 384 times larger, so whether it should be used in future research still requires careful consideration.

Compared with previous studies, the key reason why the modeling in this experiment was able to capture the relationships between variables more effectively lies in the use of a high-resolution bathymetric dataset to describe reef morphology during the data preparation stage, rather than relying on noisy remote sensing imagery in tropical regions (Sengupta, Ford et al. 2023). So, the usage of bathymetric data largely improved the design and use of reef morphology feature variables.

# 5. CONCLUSION

This study is based on the challenges faced in past reef island morphology research when applying machine learning approaches to explain the influence of historical meteorological and topographic data on local shorelines. In the experiments, nine models were developed to test and predict along-transect shoreline positions for natural reef islands in the South Maalhosmadulu Atoll, Maldives, across nine years of historical data.

From the results, tree-based ensemble learners outperformed other models in single-island, multi-island modeling, and multi-island future morphology prediction. Among them, Random Forest and Stacking achieved $R^2$ values above or close to 0.9 in all three experiments. However, the cross-island Generalization experiment showed that all models were almost unable to predict the unseen island, meaning that cross-island transferability is limited by the significant differences among islands and small number of natural islands in this study. In predicting future island morphology, Random Forest and Stacking proved capable of estimating shoreline positions near transects on trained islands for any day in the future, without relying on strict time-series structures. However, compared with Stacking and other models, Random Forest uses more than 384 times that amount.Reef width and local terrain slope were identified as the two most critical factors shaping shoreline morphology, and nearly all variables describing local reef structure ranked among the top features in contribution across all experiments. This finding is consistent with the physical principles of island formation and highlights the dominant importance of reef morphology in reef island prediction studies.

Overall, ensemble learning provides a robust framework for balancing individual, joint, and future predictive accuracy with computational efficiency in reef island morphodynamical modeling. At the same time, larger and more diverse datasets will be needed in the future to improve transferability to unseen islands.

# REFERENCE


Barnett, J., et al. (2022). "Nature-based solutions for atoll habitability." Philosophical Transactions of the Royal Society B **377**(1854): 20210124.

Christofi, D., et al. (2025). "A Review of Open Remote Sensing Data with GIS, AI, and UAV Support for Shoreline Detection and Coastal Erosion Monitoring." Appl. á Sci. á **15**: 4771.

Kench, P. S. and R. W. Brander (2006). "Response of reef island shorelines to seasonal climate oscillations: South Maalhosmadulu atoll, Maldives." Journal of Geophysical Research: Earth Surface **111**(F1).

Kench, P. S. and R. W. Brander (2006). "Wave processes on coral reef flats: implications for reef geomorphology using Australian case studies." Journal of Coastal Research **22**(1): 209-223.

Kench, P. S., et al. (2005). "New model of reef-island evolution: Maldives, Indian Ocean." Geology **33**(2): 145-148.

Kench, P. S., et al. (2024). "Island change framework defines dominant modes of atoll island dynamics in response to environmental change." Communications Earth & Environment **5**(1): 585.

LEGOS, N. a. C. a. m. f. a. b. A. (2024). FES2022 (Finite Element Solution) Tidal model (Version 2024).

Masselink, G., et al. (2020). "Coral reef islands can accrete vertically in response to sea level rise." Science advances **6**(24): eaay3656.

Masselink, G., et al. (2021). "Role of future reef growth on morphological response of coral reef islands to sea-level rise." Journal of Geophysical Research: Earth Surface **126**(2): e2020JF005749.

Meteorology, D. o. (1995). Some meteorological data 1966–1994. D. o. Meteorology.

Ortiz, A. C. and A. D. Ashton (2019). "Exploring carbonate reef flat hydrodynamics and potential formation and growth mechanisms for motu." Marine Geology **412**: 173-186.

Park, S. and A. Song (2024). "Shoreline change analysis with Deep Learning Semantic Segmentation using remote sensing and GIS data." KSCE Journal of Civil Engineering **28**(2): 928-938.

Rasheed, S., et al. (2021). "An improved gridded bathymetric data set and tidal model for the Maldives archipelago." Earth and Space Science **8**(5): e2020EA001207.

Roelvink, F., et al. (2025). "Climate adaptation for a natural atoll island in the Maldives-predicting the long-term morphological response of coral islands to sea level rise and the effect of hazard mitigation strategies." Earth's Future **13**(4): e2024EF005576.

Sengupta, M., et al. (2023). "Drivers of shoreline change on Pacific coral reef islands: linking island change to processes." Regional Environmental Change **23**(3): 110.

Sengupta, M., et al. (2025). "Exploring the drivers of reef island shoreline change using machine learning models." Scientific reports **15**(1): 16735.

Shope, J. B. and C. D. Storlazzi (2019). "Assessing morphologic controls on atoll island alongshore sediment transport gradients due to future sea-level rise." Frontiers in Marine Science **6**: 245.

Storlazzi, C. D., et al. (2018). "Most atolls will be uninhabitable by the mid-21st century because of sea-level rise exacerbating wave-driven flooding." Science advances **4**(4): eaap9741.

Vos, K., et al. (2019). "CoastSat: A Google Earth Engine-enabled Python toolkit to extract shorelines from publicly available satellite imagery." Environmental Modelling & Software **122**: 104528.

Wandres, M., et al. (2024). "A national-scale coastal flood hazard assessment for the atoll nation of Tuvalu." Earth's Future **12**(4): e2023EF003924.

Wu, M., et al. (2021). "Multi-decadal atoll-island dynamics in the Indian Ocean Chagos Archipelago." Global and Planetary Change **202**: 103519.

Young, I. R. (1999). "Seasonal variability of the global ocean wind and wave climate." International Journal of Climatology: A Journal of the Royal Meteorological Society **19**(9): 931-950.

## AI Acknowledgement Statement

This report has made use of *ChatGPT-4.5o* and *ChatGPT-5o*, developed and provided by OpenAI (https://chat.openai.com). These tools were used to assist with drafting, refining, and debugging experiments codes. All analysis, interpretations, and conclusions presented in this report are entirely my own, and I remain fully responsible for the submitted work.